Periodic versus chaotic dynamics in vibratory feeders

By M.-O. Hongler and J. Figour

Institut de Microtechnique, Département de Mécanique, E.P.F.L., CH-1015 Lausanne, Switzerland

Abstract. In mechanical engineering and more precisely in automatic assembly devices, one is faced with the problem of conveying parts to assembly locations. The transporters which are used are commonly realized in the form of vibratory feeders. Roughly speaking a vibratory feeder consists of a vibrating and guiding track on which parts to be conveyed are forced into motion. We discuss such a mechanical situation from the point of view of the theory of non-linear discrete mapping which arise naturally in this situation. While previous analysis of vibrating feeders were restricted to the purely periodic regimes, we point out here the existence of chaotic regimes which result form the non-linear dynamics; (cascade of bifurcations leading to chaotic dynamics). The transport rate of the system is studied both in the periodic and chaotic regimes.

1. Introduction

The problem of feeding parts in an automatic assembly chain is certainly not a minor aspect in the conception of a reliable system. One of the solutions which is commonly adopted is the use of vibratory transporters [1]. In its essence, a vibratory transporter, also called vibratory feeder, is constituted by an oscillating track on which the parts to be transported are disposed. When the track is set into vibrations, the mobile lying on it is itself set into movement and for vibrations which are properly tuned, the required feeding rate is reached. While the basic properties of vibratory feeding are known for a long time, its precise realizations have been accomplished only during the last 25 years. Besides the pioneering work [1] which sets the basic theoretical and experimental aspects of the question in precision engineering, without attempting to be exhaustive, let us mention Ref. [1–7] in which the reader will find refined developments together with extended biography sources. The rich literature devoted to this topic reflects the numerous problems the constructor of vibratory feeders has to deal with. Usually, a vibratory transporter is tailored for each particular application and the final tuning is achieved experimentally in very much the same way as a musical craftsman proceeds. The reader is therefore warned that this paper does not produce explicitly analytic solutions which match the general problem. Rather, we focus our attention to extract some universal qualitative features common to

most feeders. Our point of view is the one adopted in the study of non-linear dynamical systems, i.e. the search of qualitative universal features [8–10]. To our knowledge, the problem of vibratory feeders has not been yet studied from the qualitative dynamics point of view, therefore we explore our problem under the recent results obtained in the topic the non-linear dynamics.

Our paper is organized as follows: In Section 2, we introduce the mechanical system to be studied and its modelization. The dynamics is written in terms of a non-linear mapping. In Section 3, we discuss the properties of the mapping and deduce the existence of a Feigenbaum cascade of period doubling bifurcations. We also calculate the mean transport velocity on the track, a quantitity intimately related to the transport rate of the feeder itself. Finally, Section 4 is devoted to some comments.

2. The Vibratory feeder and its modelization

In actual applications, the vibratory feeders may present various geometries. The most common realizations are those presenting a bowl shape [1]. Inside the bowl, a helical guiding track conveys the parts when vibrations are turned on. In this paper, we shall focus our attention to a simpler geometry, namely the linear vibrating track. Indeed, in this particular arrangement, the centripetal and Coriolis acceleration which are to be considered in bowls, can be omitted. Therefore, the dynamics of the linear track is simpler than the one of the bowl, however its essential characteristics are preserved.

The modelization we shall discuss is sketched in Fig. 2, where the basic notations are introduced. We shall choose the *xOy* coordinate frame to be attached to the track. Accordingly, the general equations of the motion for a part
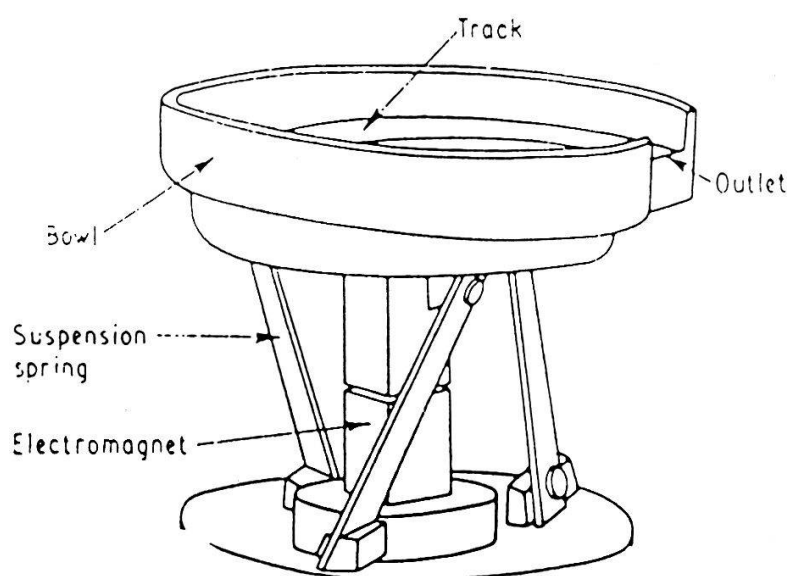

Figure 1
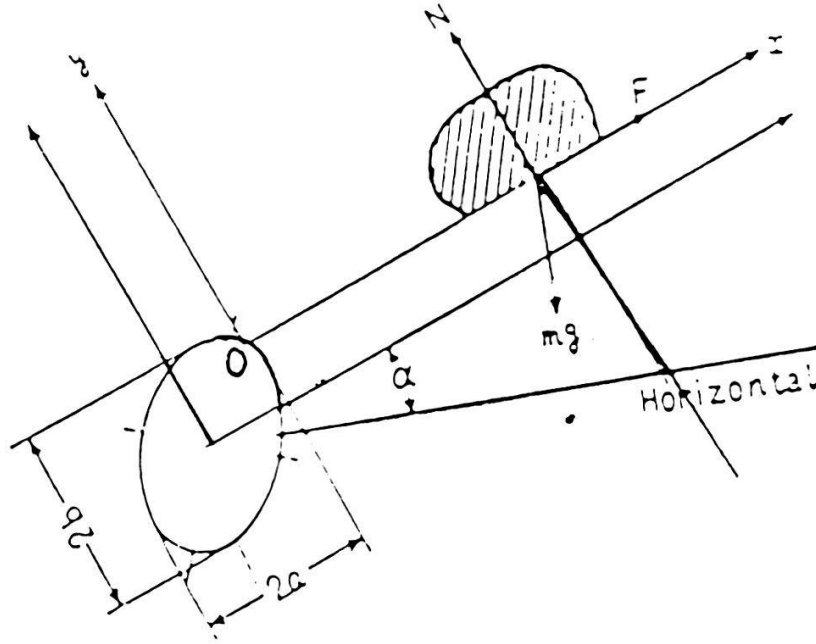Typical realization of a vibratory feeder.

Figure 2
Schematic view of the dynamical system.

of mass m can be written under the form [2]:

$$m \frac{d^2}{dt^2} x(t) = ma\omega^2 \sin(\omega t + \gamma) - mg \sin(\alpha) + F \tag{1a}$$

$$m \frac{d^2}{dt^2} y(t) = mb\omega^2 \sin(\omega t) - mg \cos(\alpha) + N \tag{1b}$$

where, F and N stand respectively for the friction and constraint forces, α is the angle of the track with the horizontal (see Fig. 2), g the gravitational acceleration and γ the phase shift between the parallel and perpendicular components of the excitation of the track. The fact that the amplitudes of the parallel and perpendicular components of the excitation are not equal $(a \neq b)$, indicates that we consider generally elliptical vibrations.

Depending on the actual values of F and N, the motion of the mobile can be either of the sliding type (S-regime), of the hopping type (H-regime), or a combination of both sticking and hopping regimes, (H-S regimes).

Different possible scenarios, always based on a periodic motion of the conveyed parts, are presented in Ref. [1, 5]. Here, we shall focus our attention to the H-regime which is the situation one has to deal with when high transport rates are required [1]. The H-regime will always be reached for relatively large (see below for a more quantitative specification) excitation parameters.

In the pure H-regime and between the impacts with the track, the equations of the motion equations (1a, b) simply reduce to the free flight equations. In

other words, we shall have:

$$\frac{\partial^2}{\partial \tau^2} u(\tau) = \sin(\tau) - k \tag{2a}$$

$$\frac{\partial^2}{\partial \tau^2} v(\tau) = \eta \sin(\tau + \gamma) - k + g(\alpha) \tag{2b}$$

where in equations (2a, b) the dimensionless parameters introduced are defined as:

$$k = g \cos(\alpha)/b\omega^2; \qquad \eta = a/b; \qquad \tau = \omega t$$

$$u = y/b; \qquad v = x/a. \tag{3}$$

Between the impacts, equations (2a, b) completely describe the dynamics of the system. Let us now focus our attention at one of the impacts which we shall assume occurs at time $\tau = \tau_n$. We shall specify the impact dynamics by the following restitution equations:

$$\left.\frac{\partial u}{\partial \tau}\right|_{\tau = \tau_n + \varepsilon} = -R_\perp \left.\frac{\partial u}{\partial \tau}\right|_{\tau = \tau_n - \varepsilon} \tag{4a}$$

$$\left.\frac{\partial v}{\partial \tau}\right|_{\tau = \tau_n + \varepsilon} = R_\| \left.\frac{\partial v}{\partial \tau}\right|_{\tau = \tau_n - \varepsilon} \tag{4b}$$

where the coefficients of the perpendicular (parallel) restitution are denoted respectively by $R_\perp$, $(R_\|)$ and ε is vanishingly small quantity relating times just before and after impact at time $\tau = \tau_n$. Obviously we have:

$$0 \le R_\perp \le 1 \quad \text{and} \quad 0 \le R_\| \le 1 \tag{5}$$

Now, let us introduce the following notations:

$$\left.\frac{\partial u}{\partial \tau}\right|_{\tau = \tau_n} = \psi_n \quad \text{and} \quad \left.\frac{\partial v}{\partial \tau}\right|_{\tau = \tau_n} = \phi_n \tag{6}$$

Renewing the initial conditions each time an impact occurs, we integrate equations (2a, b) and use the notation equation (6) and get:

$$\frac{\partial u}{\partial \tau} = -k(\tau - \tau_n) + \cos(\tau_n) + \psi_n - \cos(\tau) \tag{7a}$$

$$u(\tau) = \frac{-k}{2}(\tau - \tau_n)^2 + [(\cos(\tau_n) + \psi_n](\tau - \tau_n) - [\sin(\tau) - \sin(\tau_n)] \tag{7b}$$

and

$$\frac{\partial v}{\partial \tau} = -\eta[\cos(\tau + \gamma) - \cos(\tau_n + \gamma) - ktg(\alpha)(\tau - \tau_n) + \phi_n] \tag{7c}$$

Expressing the fact that $u(\tau_{n+1}) = 0$ when the impact τ_{n+1} occurs, we can

immediately derive the relation:

$$\frac{-k}{2}(\tau_{n+1} - \tau_n)^2 + [\cos(\tau_n) + \psi_n](\tau_{n+1} - \tau_n) = \sin(\tau_{n+1}) - \sin(\tau_n). \tag{8}$$

Finally, from the impact relations equations (4a, b), we obtain:

$$\psi_{n+1} = R_\perp \{k(\tau_{n+1} - \tau_n) + \cos(\tau_{n+1}) - \cos(\tau_n) - \psi_n\} \tag{9}$$

$$\phi_{n+1} = R_\parallel \{ -\eta[\cos(\tau_{n+1} + \gamma) - \cos(\tau_n + \gamma) - ktg(\alpha)(\tau_{n+1} - \tau_n) + \phi_n\} \tag{10}$$

The non-linear, discrete mapping equations (8)–(10) fully characterizes the dynamics of our mechanical systems. We may emphasize, that to write the dynamics, we implicitly assumed that the impacts of the mobile do not alter the motion of the track itself. This assumption is reasonable for most situations.

We close this chapter in calculating the transport rate of our vibratory feeder. This quantity is directly related to the mean velocity W_n (in the parallel direction) achieved between two successive impacts. Using equation (7c), we may write:

$$W_n = \frac{1}{\tau_{n+1} - \tau_n} \int_{\tau_n}^{\tau_{n+1}} \left(\frac{\partial}{\partial \tau} v(\tau)\right) d\tau$$

$$= [\eta \cos(\tau_n + \gamma) + \phi_n] - \frac{k}{2} tg(\alpha)(\tau_{n+1} - \tau_n) \tag{11}$$

$$- \frac{\eta}{\tau_{n+1} - \tau_n} [\sin(\tau_{n+1} + \gamma) - \sin(\tau_n + \gamma)]$$

As far as the formulation is concerned, the dynamical problem is completely specified by equations (8)–(11). Indeed, given the initial conditions τ_0, Φ_0 and Ψ_0, we may iterate the mapping and then calculate W_n.

3. Discussion of the dynamics

Now, we study the properties of the mapping derived in Section 2. First, let us observe that equation (10) is decoupled from equation (8) and (9). Hence we can first confine our discussion to these last equations. Being transcendental, equation (8) cannot be solved analytically for τ_n. Equation (8) and (9) admit the general form:

$$\tau_{n+1} = f_1(\tau_n, \psi_n) \tag{12a}$$

$$\psi_{n+1} = f_2(\tau_n, \psi_n) \tag{12b}$$

where both f_1 and f_2 are non-linear functions.

Recently, the mapping equations (8) and (9) have stimulated research both from the theoretical [9–13] and the experimental [12, 15] point of view. In these references, the problem of a bounding ball on a vibrating table is studied and in

our problem equations (8) and (9) precisely describe the same situation. Hence, we shall largely use the results already established which we recall here briefly.

a) The mapping equations (8) and (9) present both periodic and chaotic solutions. The occurrence of these regimes are governed by changing the external control parameters k and $R_\perp$ (see equations (3) and (5)).

b) The transition from periodic solutions to a chaotic regime occurs via the famous Feigenbaum cascade of bifurcations. This is a well known scenario to approach the deterministic chaos.

Let us now come to a more detailed analysis by considering various values of the control parameter k. Here, we assume $R_\perp$ to be fixed.

Sticking regime

In view of equations (2a, b) and (8), when $k > 1$ the mobile sticks to the track for an initial condition on the track itself. For an initial condition off the track, the sticking regime will finally be reached after a sufficient number of jumps occurred. Indeed, for each impact with the track, energy is dissipated via the impact relation equation (5). In this regime, the transport of parts can also be realized. It is due in this case only to the inertia of the mobile. Of course, this regime is characterized by an ad-hoc excitation force which is asymmetric with time.

Hopping regime

In this case the parameter $k < 1$. First let us focus our attention to the periodic case:

Periodic & hopping regime

Introducing the Ansatz:

$$\tau_{n+1} = \tau_0 + r(2\pi n) \qquad \begin{matrix} r \in \mathbb{N} \\ r \in \mathbb{N} \end{matrix} \tag{13}$$

we may derive the necessary condition for the existence of a periodic solution.

The Ansatz equation (13) indicates that we are here interested in periodic solutions with period one; (The Ansatz for a period k relates τ_{n+k} with τ_n). Introducing equation (13) into equations (8) and (9), the necessary conditions for a period one orbit read as:

$$\psi_{n+1} = \psi_n = \psi = \frac{(2\pi r k) R_\perp}{1 + R_\perp} \tag{14a}$$

$$\tau_0 = A \cos\left\{\pi r k \left(\frac{1 - R_\perp}{1 + R_\perp}\right)\right\} \tag{14b}$$

The existence of a real τ_0 implies immediately:

$$k \leq \frac{1}{\pi r}\left(\frac{1+R_\perp}{1-R_\perp}\right) = k_{1,r} \tag{15}$$

The stability of the above solution, which is a fixed point of the mapping equations (8) and (9), is determined by the behavior of the eigenvalues of the linearized mapping around (Ψ, τ_0). This calculation is performed in [12] where it is established that the periodic solutions equations (14a, b) are stable with period one when:

$$\tau_0 \leq Atg\left\{\frac{2}{\pi}\left(\frac{1+R_\perp^2}{1-R_\perp^2}\right)\right\} \tag{16}$$

Using equations (14b) and (16), we may express the stability condition on the parameter k itself which is the unique parameter which controls the tuning of the feeder; (remember that $T_\perp$ is fixed once the mobile has been chosen).
We end with the case where:

$$k \geq \left[\pi^2\left(\frac{1-R_\perp}{1+R_\perp}\right) + 4\frac{(1+R_\perp^2)}{(1+R_\perp)^4}\right]^{-1/2} = k_{2,1} \tag{17}$$

In the general case, a similar expression is given in [2, 11] and reads:

$$k \geq \left[\pi^2 r^2\left(\frac{1-R_\perp}{1+R_\perp}\right)^2 + 4\frac{(1+R_\perp^2)^2}{(1+R_\perp)^4}\right]^{-1/2} = k_{2,r} \tag{17a}$$

Hence, equations (15) and (16) determines bands of values for the control parameter k where stable period one solutions arise.

$$k_{1,r} \geq k \geq k_{2,r} \tag{18}$$

Typical values for an actual application would be: $\omega = 2\pi * 50\,\mathrm{s}^{-1}$; $g = 9.81\,\mathrm{m/s}^2$; $R_\perp = 0.2$ which yields:

$r = 1$ $0.3928 \leq b^{-1}\cos(\alpha) \leq 0.4774$

$r = 2$ $0.2213 \leq b^{-1}\cos(\alpha) \leq 0.2387$

$r = 3$ $0.1551 \leq b^{-1}\cos(\alpha) \leq 0.1591$

where b is expressed in meters $* 10^{-4}$. These values can be experimentally checked using the simulation [15].

Let us now discuss what happens when the parameters k is decreased below $k_{2,r}$. (see Ref. [9, 11, 12]). When $k < k_{2,r}$, a stable periodic motion occurs with a period which is the double of the fundamental one. This behavior is observed until a value $k_{3,r} < k_{2,r}$ is reached where again a stable motion is generated with a period which is again the double of the previous one. This sequence continues until a value $k_{1,\infty}$ is reached beyond which a chaotic motion is observed. The

succession of the bifurcation values obeys the formula [16]:

$$\lim_{\nu \to \infty} \frac{k_{\nu+1,r} - k_{\nu,r}}{k_{\nu+2,r} - k_{\nu+1,r}} = 0.46992 \tag{19}$$

While for $k > 1$ the motion is in the S-regime, for $k_{1,r} < k < 1$, the motion consists in a mixture of $H\&S$-regimes (see Ref. [1] for a detailed description of peridic $H\&S$-regimes). Schematically, we may summarize the situation by the diagram sketched in Fig. 3 [11, 14]. This behaviour is the Feigenbaum cascade of bifurcations and is one of the standard routes to chaotic regimes [10] which can be encountered in numerous non-linear dynamical systems.
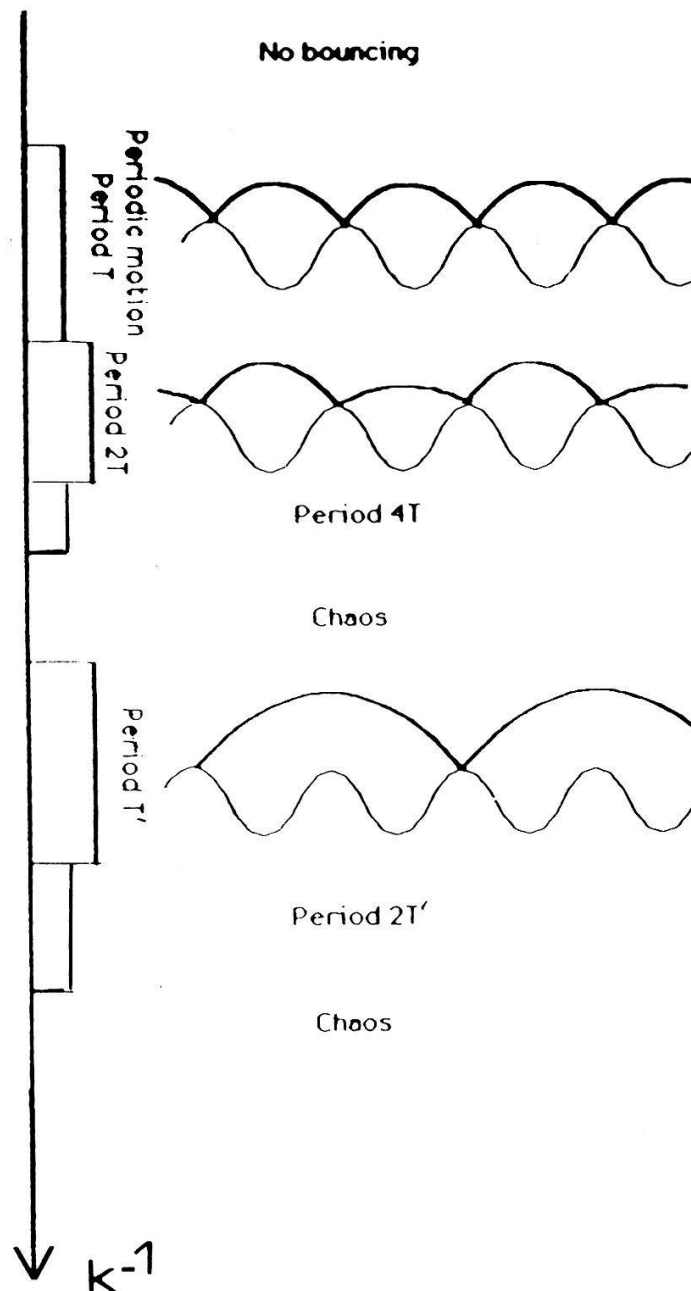

Figure 3
Sketch of the various synamical regimes.

Let us now calculate the various transport rates obtained in the different vibrating regimes of our system. In the periodic situations specified by equations (14a, b), equation (11) immediately implies:

$$W_n = W = \eta \cos(\tau_0 + \gamma) - k\pi r tg(\alpha)\left(\frac{1 + R_{\|}}{1 - R_{\|}}\right) \tag{20}$$

When $\gamma = 0$, which is the common situation in industrial realizations, we may use equations (14b) to get:

$$W = \pi r k\left[\eta\left(\frac{1 - R_\perp}{1 + R_\perp}\right) - tg(\alpha)\left(\frac{1 + R_{\|}}{1 - R_{\|}}\right)\right] \tag{21}$$

In particular, we may deduce from equation (20) the critical slope of the track for which the motion reverses it direction. We have:

$$\alpha_e = Atg\left\{\eta\frac{(1 - R_\perp)(1 - R_{\|})}{(1 + R_\perp)(1 + R_{\|})}\right\} \tag{22}$$

When γ is non-vanishing, the general expression for the mean transport velocity reads:

$$W = \pi r k\left[\eta\cos(\gamma)\left(\frac{1 - R_\perp}{1 + R_\perp}\right) - tg(\alpha)\left(\frac{1 + R_{\|}}{1 - R_{\|}}\right)\right]$$
$$- \eta\sin(\gamma)\left[1 - \pi^2 k^2 r^2\left(\frac{1 - R_\perp}{1 + R_\perp}\right)^2\right]^{1/2} \tag{23}$$

We now turn our attention to the transport rate obtained when the feeder operates in the chaotic regime.

We first rewrite equation (10) in the form:

$$W_n = \eta\cos(\tau_n + \gamma) - \frac{k}{2}tg(\alpha)(\tau_{n+1} - \tau_n) + \phi_n$$
$$- \frac{\eta\cos(\gamma)}{\tau_{n+1} - \tau_n}[\sin(\tau_{n+1}) - \sin(\tau_n)]$$
$$- \frac{\eta\sin(\gamma)}{\tau_{n+1} - \tau_n}[\cos(\tau_{n+1}) - \cos(\tau_n)]. \tag{24}$$

Using equation (8) into equation (24), we obtain:

$$W_n = [\phi_n - \eta\cos(\gamma)\psi_n] + (\tau_{n+1} - \tau_n)\left[\frac{\eta k}{2}\cos(\gamma) - \frac{k}{2}tg(\alpha)\right]$$
$$- \eta\sin(\gamma)\sin(\tau_n) - \frac{\eta\sin(\gamma)}{\tau_{n+1} - \tau_n}[\cos(\tau_{n+1}) - \cos(\tau_n)] \tag{25}$$

It will be also useful to express Φ_n and Ψ_n directly in term of their initial conditions Φ_0 and Ψ_0. This is deduced by a direct iteration of equations (9) and

(10):

$$\phi_n = R_{\parallel}^n \phi_0 + R_{\parallel}^n \sum_{l=0}^{n-1} R_{\parallel}^{-l} [-ktg(\alpha)(\tau_{l+1} - \tau_l) - \eta \delta(\tau_l)] \tag{26a}$$

$$\psi_n = (-R_{\perp})^n \psi_0 + (-R_{\perp}) \sum_{l=0}^{n-1} (-R_{\perp})^{-l} [k(\tau_{l+1} - \tau_e) - \delta(\tau_l)] \tag{26b}$$

where:

$$\delta(\tau_l) = \cos(\tau_{l+1}) - \cos(\tau_l) \tag{27}$$

Now, we observe that when n grows to large values, a stationary regime will be reached. Indeed due to the dissipation of energy (see equation (5)), the initial condition is lost. In the chaotic regime, the interimpact time $z_l = (\tau_{l+1} - \tau_l)$ form a random non-negative sequence. We shall assume that in the chaotic regime, we may approximate the stochastic process z to be a renewal process [17, 18], i.e. the z_l are independent and identically distributed with a distribution F. Under these assumptions, we can write [17, 18]:

$$\tau_n = \sum_{l=0}^{n-1} z_l; \qquad (\tau_0 = 0) \tag{28}$$

and therefore τ_n is distributed with the law $F_n^*(z)$ which is the n-fold convolution of the distribution $F(z)$; [17, 18].

Considering very large n, let us now take the mean of equation (24).

$$\langle W_n \rangle = \langle \phi_n \rangle - \eta \cos(\gamma) \langle \psi_n \rangle + \Delta \left\{ \frac{\eta k}{2} \cos(\gamma) - \frac{k}{2} tg(\alpha) \right\}$$

$$- \eta \sin(\gamma) < \sin(\tau_n) > - \eta \sin(\gamma) \left\langle \frac{\cos(\tau_{n+1}) - \cos(\tau_n)}{\tau_{n+1} - \tau_n} \right\rangle \tag{29}$$

where:

$$\Delta = \int_{R^+} dF(z)z \tag{30}$$

denotes the mean inter-impact time. Furthermore, the use of equations (26a) and (26b) enables to write:

$$\langle \phi_n \rangle_{n \gg 1} \cong \frac{-ktg(\alpha)R_{\parallel}}{1 - R_{\parallel}} \Delta - \eta R_{\parallel}^n \sum_{l=0}^{n-1} \frac{\langle \delta(\tau_l) \rangle}{(R_{\parallel})^l} \tag{31a}$$

$$\langle \psi_n \rangle_{n \gg 1} \cong \frac{kR_{\perp}}{1 + R_{\perp}} \Delta + (-R_{\perp})^n \sum_{l=0}^{n-1} \frac{\langle \delta(\tau_l) \rangle}{(-R_{\perp})^l} \tag{31b}$$

where:

$$\langle \delta(\tau_l) \rangle = \int_{R^+} \cos(z) [dF_{l+1}^*(z) - dF_l^*(z)]. \tag{32}$$

Then, we obtain from equation (25) and for the situation $\gamma = 0$; we obtain:

$$\langle W_n \rangle \cong \frac{k\Delta}{2}\left[\eta\left(\frac{1 - R_\perp}{1 + R_\perp}\right) - tg(\alpha)\left(\frac{1 + R_\parallel}{1 - R_\parallel}\right)\right]$$

$$-\left\{\eta \int_{R^+} \sum_{l=0}^{n-1} [R_\parallel^{n-l} - (-R_\perp)^{n-l}](dF_{l+1}^*(z) - dF_l^*(z))\cos(z)\right\}$$

$$(33)$$

Remark. Equation (33) immediately restitutes the result equation (23) when the motion is periodic. Indeed, in this case, the expression in the curly bracket in equation (33) is identically vanishing and Δ obviously equals $2\pi r$.

From equation (33), we deduce that the crucial quantity to calculate the transport is the mean inter-impact time Δ. The longer Δ is, the larger the transport rate of the feeder will be. Of course, to calculate Δ and the influence of the curly bracket term in equation (33) one has to derive rigourously the probability distribution $F(z)$ from the basic dynamics itself; we are not yet able to perform such a derivation in the general case.

To estimate the mean conveying rate, we shall assume that the term in the curly bracket in equation (33) can approximately be neglected. Indeed, the mean conveying rate will be given by:

$$W = \lim_{N \to \infty} \frac{1}{N} \sum_{n=N}^{2N} W_n = \approx \frac{k\Delta}{2}\left[\eta\left(\frac{1 - R_\perp}{1 + R_\perp}\right) + tg(\alpha)\left(\frac{1 + R_\parallel}{1 - R_\parallel}\right)\right]. \qquad (34)$$

where precisely we have dropped the curly bracket which is likely to exhibit an oscillating behaviour and will therefore approximately disappear through the averaging procedure. Hence, to first approximation, the mean conveying rate depends on the mean inter-impact time, the asymmetry in the excitation η, the slope of the track α the restitution coefficient $R_\perp$ & $R_\parallel$ and the amplitude of the excitation k.

We can now estimate the maximum transport rate attained by the feeder. In Ref. [13], the velocity Ψ_n is shown to be confined to the srip; ($A^*\omega$ in the notation of [13] is here equal to 1):

$$|\psi| < \frac{1 + R_\perp}{1 - R_\perp} \qquad (35)$$

and hence if we estimate the interimpact time as being given by the free flight time, we have:

$$\tau_{n+1} - \tau_n \simeq \frac{2\psi_n}{k} = \frac{1}{k}\left(\frac{1 + R_\perp}{1 - R_\perp}\right) \qquad (36)$$

Introducing finally equation (36) into equation (34), we end with:

$$W < W_{max} = \eta\left(1 - \frac{tg(\alpha)}{tg(\alpha_c)}\right) \qquad (37)$$

where α_c has already been defined in equation (22).

Remark that W_{max} is indeed bounded by η which indicates that the approximations performed are consistent. It is finally also interesting to consider the limiting case for which $R_\perp$ & $R_\parallel$ are vanishingly small. In this case equation (25), with the choice $\gamma = 0$, becomes:

$$W_n = (\tau_{n+1} - \tau_n)\left[\frac{3k}{3}\cos(\gamma) - \frac{k}{2}tg(\alpha)\right] \tag{38}$$

For this limiting case, equation (9) with $\Phi_n = 0$, determines itself completely the successive impact times τ_n. As mentioned in Ref. [11], where an approximate version of the mapping equation (9) is discussed, the situation is closely related to the one-dimensional quadratic map of the interval studied in Ref. [16] which also exhibits the Feigenbaum cascade of bifurcations. Here again, the probability distribution $F(z)$ is to be calculated from the basic dynamical equations of the motion. In particular, it could be taken as the invariant distribution of the mapping [8]. While this quantity can be determined by numerical calculations for any particular values of k, analytical expressions are generally impossible to obtain [8].

4. Conclusions

We have modelized the dynamics of vibratory feeder under the form of a linear vibrating track. The regimes considered are restricted to the situation where the mobile jumps on the track. In this case, we deduce that the motion of the conveyed particle in the feeder can be either periodic or chaotic according to the value of the external control parameter which tunes the device; (here this parameter is a combination of the frequency and the amplitude of the vibrations of the track). The chaotic regime is intrinsic to the dynamics and therefore is not generated by the presence of external mechanical noise. The transition from the periodic regime (whose range of stability is examined) to the chaotic one is observed to obey a cascade of bifurcations of the Feigenbaum type (period doubling cascade of bifurcations). Of course, in the actual feeder, the cascade of bifurcations will be truncated and the chaotic regime will be attained soonly. This effect is due to the ubiquous presence of noise sources and is confirmed from the experiments carried in Ref. [12], where a very similar dynamical system has been investigated. As the range of values of the control parameter which leads to chaotic behaviour is much wider than the strips in which a purely periodic regime is possible (this even when external noise is omitted in the analysis) tends to indicate that actual feeders are likely to operate chaotically in the jumping regime (i.e. when a high feeding rate is required). Furthermore, we have also estimated the feeding rate of our device both in the purely periodic regime and in the chaotic one. We have to point out that the present first approach has been carried out with a purely sinusoidal excitation force of the track. In actual feeders, the excitations can in fact be more complicated. Along these lines, a superposition of two sinusoidal excitations for the bouncing ball problem has been considered in [19]. As a result, shifts of the bifurcation points are observed, however chaotic solutions always exist.

To conclude, we should like to stress that in the study of vibratory feeding the presence of chaotic solutions have to be considered systematically when the jumping regime is switched on. Indeed, chaotic motions are in fact expected for a large range of external parameters. Hence, the analysis of purely periodic solutions of the non-linear dynamical mappings is not sufficient to discuss the behaviour of the system properly. Moreover, the presence of external noise in actual feeders will further reduce the range of parameters for which periodic solutions are possible. Therefore, rather than considering the chaotic solutions as artifacts to be avoided, they would be taken as being the rule in feeders which operate in the hopping regime. Concerning the transport rate in the chaotic regime, further studies are required and are presently in progress. Let us stress here that far from being a drawback, the chaotic solutions will in fact give rise to transport rate which are not too sensitive to the variations of the external excitation parameters. This observation which has already been reported in [7] (on the basis of computer simulation), leads to the conclusion that chaos will in fact constitute an advantage. This permits to expect a feeding rate which is more or less independent of variations of excitations, variations which are unavoidable and constitute one of the difficulties inherent to any installation.

Let us finally emphasize that the type of device described here bridges the gap between two types of transport mechanisms, namely: a purely deterministic one, (such as periodic regimes of the feeder) and a purely stochastic one, (such as pure diffusion processes). Indeed, while the basic equations of the motion are purely determinsitic, the transport properties of the feeder are governed by the pseudo-stochastic solutions of the non-linear dynamics. This situation needs not necessarily to be restricted to the 'vibratory feeder', but certainly arises in other physical contexts where the transport is induced by periodic external forces.

REFERENCES

[1] A. H. REDFORD and G. BOOTHROYD. *Vibratory Feeding* Proc. Instn. Mech Engrs. *182*, 135, (1967–68).
[2] J. INOUE, S. MIYAURA and A. NISHIYAMA. *On the vibroseparation and vibrotransportation.* Bull. of the J.S.M.E. *11*, 102, (1968).
[3] Y. JIMBO, Y. YOKOHAMA and S. OKABE. *Study of vibratory conveying.* Int. Conf on Production Eng. Tokyo (1974).
[4] S. OKABE, K. KAMIYA, K. TSUJIKADO and Y. YOKOYAMA. *Vibratory feeding by non-sinusoidal vibratory optimum wave form.* Trans of the A.S.M.E. *107*, 188, (1985).
[5] O. TANIGUCHI, J. SAKATA, Y. SUZUKI and Y. OSANAI. *Studies on vibratory feeder.* Bull. J.S.M.E. *6*, 37, (1963).
[6] V. L. VEITZ and I. SH. BEILIN. *Dynamics of transportation of a material particle with stochastic characteristic along a horizontal plane.* Mechanism and Machine Theory 7, 155, (1972).

[7] YA. F. VAYNKOF and S. V. INOSOV. *Non-periodic motion in vibratory conveying in states of operation accompanied by throwing.* Mechanical Sciences – Maschinovedeniye *5*, 1, (1976).

[8] A. J. LICHTENBERG and M. A. LIEBERMAN. *Regular and stochastic motion.* Applied Math Sciences *38* (1983); Springer.

[9] J. GUCKENHEIMER and P. HOLMES. *Non-linear oscillations, dynamical systems and bifurcations of vector fields.* Applied Math. Sciences *42*, (1983); Springer.

[10] L. O. CHUA, *Special Issue on Chaotic Systems.* Proc. of the IEEE. *75* (1987).

[11] P. J. HOLMES, *The dynamics of repeated impacts with a sinusoidally vibrating table.* J of Sound & Vibrations *84*, 173, (1982).

[12] N. B. TUFILLARO, T. M. MELLO, Y. M. CHOI and A. M. ALBANO. *Period doubling boundaries of a bouncing ball.* J. Physique *47*, 1477, (1986).

[13] C. N. BAPAT, S. SANKAR and N. POPPLEWELL. *Repeated impacts on a sinusoidally vibrating table reappraised.* J. of Sound & Vibrations *108*, 99, (1986).

[14] N. B. TUFILLARO and A. M. ALBANO. *Chaotic dynamics of a bouncing ball.* Am J. of Phys. *54*, 939, (1986).

[15] N. B. TUFILLARO and M. ABBOTT. *Bouncing ball simulation for the McIntosch Computer.* (1988).

[16] P. COLLET and J.-P. ECKMANN. *Iterated maps on the interval as dynamical systems.* (1980). Birkhäuser Boston MA.

[17] W. FELLER. *An introduction to probability theory and its applications.* (1966); J. Wiley.

[18] S. M. ROSS. *Stochastic processes.* (1983), J. Wiley.

[19] K. WIESENFELD and N. B. TUFILLARO. *Suppression of period doubling in the dynamics of a bouncing ball.* Physica *26D*, 321, (1987).